

Identification of Specific Ligand–Receptor Interactions That Govern Binding and Cooperativity of Diverse Modulators to a Common Metabotropic Glutamate Receptor 5 Allosteric Site

Karen J. Gregory,^{†,‡,‡,#,▽} Elizabeth D. Nguyen,^{§,▽} Chrysa Malosh,^{†,‡} Jeffrey L. Mendenhall,^{||} Jessica Z. Zic,^{†,‡} Brittney S. Bates,^{†,‡} Meredith J. Noetzel,^{†,‡} Emma F. Squire,^{†,‡} Eric M. Turner,^{†,‡} Jerri M. Rook,^{†,‡} Kyle A. Emmitte,^{†,‡,||} Shaun R. Stauffer,^{†,‡,||} Craig W. Lindsley,^{†,‡,||} Jens Meiler,^{*,†,§,||,⊥} and P. Jeffrey Conn^{*,†,‡}

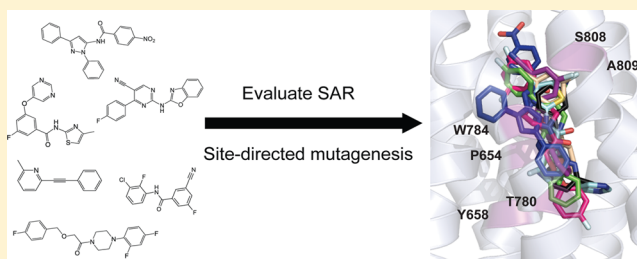
[†]Department of Pharmacology, [‡]Vanderbilt Center for Neuroscience Drug Discovery, [§]Center for Structural Biology, ^{||}Department of Chemistry, and [⊥]Institute for Chemical Biology, Vanderbilt University Medical Center, Nashville, Tennessee 37232, United States

[#]Drug Discovery Biology, Monash Institute of Pharmaceutical Sciences, Monash University, Parkville, VIC 3052, Australia

S Supporting Information

ABSTRACT: A common metabotropic glutamate receptor 5 (mGlu₅) allosteric site is known to accommodate diverse chemotypes. However, the structural relationship between compounds from different scaffolds and mGlu₅ is not well understood. In an effort to better understand the molecular determinants that govern allosteric modulator interactions with mGlu₅, we employed a combination of site-directed mutagenesis and computational modeling. With few exceptions, six residues (P654, Y658, T780, W784, S808, and A809) were identified as key affinity determinants across all seven allosteric modulator scaffolds. To improve our interpretation of how diverse allosteric modulators occupy the common allosteric site, we sampled the wealth of mGlu₅ structure–activity relationship (SAR) data available by docking 60 ligands (actives and inactives) representing seven chemical scaffolds into our mGlu₅ comparative model. To spatially and chemically compare binding modes of ligands from diverse scaffolds, the ChargeRMSD measure was developed. We found a common binding mode for the modulators that placed the long axes of the ligands parallel to the transmembrane helices 3 and 7. W784 in TM6 not only was identified as a key NAM cooperativity determinant across multiple scaffolds, but also caused a NAM to PAM switch for two different scaffolds. Moreover, a single point mutation in TMS, G747V, altered the architecture of the common allosteric site such that 4-nitro-*N*-(1,3-diphenyl-1*H*-pyrazol-5-yl)benzamide (VU29) was noncompetitive with the common allosteric site. Our findings highlight the subtleties of allosteric modulator binding to mGlu₅ and demonstrate the utility in incorporating SAR information to strengthen the interpretation and analyses of docking and mutational data.

KEYWORDS: Mutagenesis, metabotropic glutamate receptor 5, structure–activity relationships, operational model, cooperativity, affinity



Glutamate, a primary excitatory neurotransmitter within the mammalian central nervous system, mediates its effects via interactions with ionotropic and metabotropic glutamate receptors.¹ The metabotropic glutamate receptors (mGlu) are a family of eight subtypes (mGlu₁–mGlu₈) that belong to family C seven transmembrane-spanning G protein-coupled receptors (7TMR). Based on physiology and pathophysiology, metabotropic glutamate receptor subtype 5 (mGlu₅) is an attractive therapeutic target for a range of CNS-related disorders including cognitive disorders, Fragile X Syndrome, anxiety, depression, Parkinson's disease, and schizophrenia, among others.²

However, selective targeting of mGlu₅ has been a challenge as the glutamate-binding (orthosteric) site is highly conserved across all mGlu subtypes. An alternative and highly successful approach is to target allosteric binding sites that are

topographically distinct from the orthosteric site.^{3,4} The first of these so-called allosteric modulators to be discovered for mGlu₅ was MPEP.^{5,6} Allosteric modulators have the potential to enhance (positive allosteric modulators or PAMs) or inhibit (negative allosteric modulators or NAMs) the response to glutamate. A third category, silent (or neutral) allosteric modulators (SAMs), occupy allosteric sites but do not alter receptor activity. The magnitude and direction of allosteric modulation is referred to as cooperativity. In addition, multiple mGlu PAM scaffolds also exhibit intrinsic agonist activity in the absence of glutamate and such compounds are referred to as

Received: December 14, 2013

Revised: February 8, 2014

Published: February 16, 2014

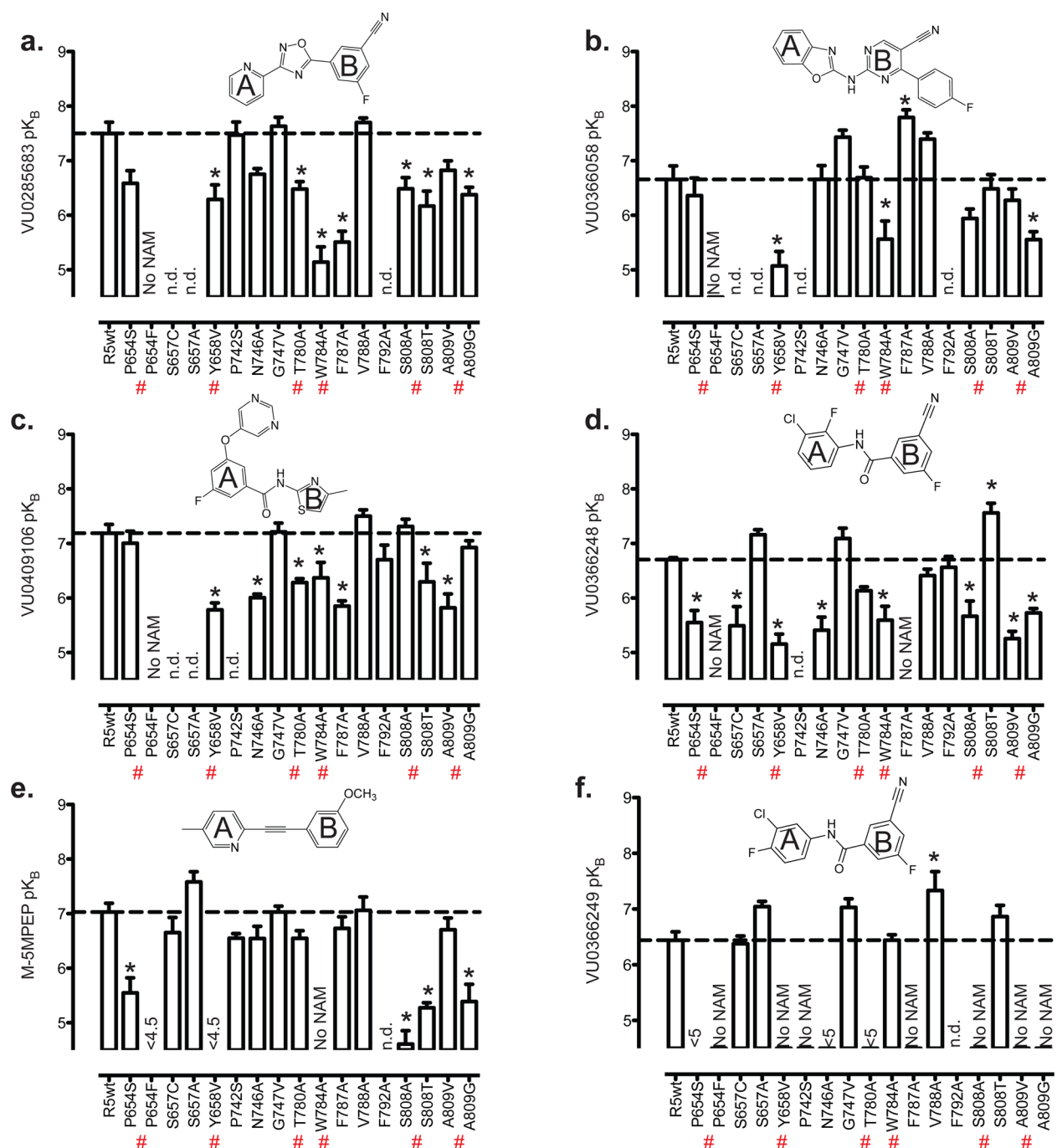


Figure 1. Allosteric modulator affinity estimates at mutant mGlu₅ constructs. Progressive modulator-induced shifts in the glutamate concentration response curve for calcium mobilization were quantified with the operational model of allosterism to estimate affinity for (a) VU0285683, (b) VU0366058, (c) VU0409106, (d) VU0366248, (e) M-5MPEP, and (f) VU0366249. Data represent mean \pm SEM of a minimum of three independent experiments, unless indicated otherwise (Supporting Information table). * indicates significantly different to wild type value, $p < 0.05$, one-way ANOVA with Dunnett's post-test. n.d. indicates not determined. "No NAM" indicates no inhibition of the glutamate response was observed up to 10 μ M of modulator. # denotes key determinant residue identified from mutagenesis. To facilitate understanding of ligand superimposition in subsequent figures, aryl rings are denoted as either "A" or "B".

ago-PAMs.⁷ At the ligand–receptor interaction level, what governs modulator affinity versus cooperativity and/or agonism remains to be fully appreciated.

In addition to increased subtype selectivity, allosteric modulators offer multiple theoretical advantages over competitive orthosteric ligands. Modulators that are quiescent in the absence of the endogenous agonist have the potential for spatial and temporal modulation of receptor function and

therefore are able to 'fine-tune' receptor activity when the endogenous agonist is present. This is a particularly attractive feature for a CNS target as 'fine-tuning' neurotransmission may yield a better therapeutic outcome than sustained activation or blockade. Moreover, the cooperativity between the two sites is saturable, such that allosteric modulators reach a 'ceiling level' to their effect that could provide a larger therapeutic index.

Table 1. Structure-Activity Relationships for mGlu₅ Negative Allosteric Modulators from Four Diverse Scaffolds Chosen for This Study^a

allosteric ligand	ID	Conf ^b	IC ₅₀ (nM)	ref
acetylene NAM (MPEP) series				
3-((6-methylpyridin-2-yl)ethynyl)benzotrile	1A	76	0.4	27
2-methyl-4-((6-phenylpyridin-3-yl)ethynyl)thiazole	1B	13	0.5	47
2-((3-methoxyphenyl)ethynyl)-6-methylpyridine	1C	571	8	28
2-methyl-6-((5-phenylpyridin-3-yl)ethynyl)pyridine	1D	21	20	48
2-methyl-6-(phenylethynyl)pyridine	1E	735	9	25
2-((2,5-dimethoxyphenyl)ethynyl)-6-methylpyridine	1F	7	82	28
2-((3-methoxyphenyl)ethynyl)-5-methylpyridine	1G	459	114	13
2-methoxy-6-(phenylethynyl)pyridine	1H	651	1961	28
methyl 2-(3-((6-methylpyridin-2-yl)ethynyl)phenoxy)acetate	1I	553	2400	48
3-((6-methylpyridin-2-yl)ethynyl)phenyl 4-methylbenzenesulfonate	1J	82	>10 000	48
<i>N</i> -aryl benzamide NAM (VU0366248) series				
2-cyano-4'-fluoro- <i>N</i> -(6-methylpyridin-2-yl)-[1,1'-biphenyl]-4-carboxamide	2A	11	5	29
2-cyano- <i>N</i> -(6-methylpyridin-2-yl)-[1,1'-biphenyl]-4-carboxamide	2B	10	14	29
<i>N</i> -(3-chlorophenyl)-3-cyano-5-fluorobenzamide	2C	8	45	42
3-cyano- <i>N</i> -(6-ethylpyridin-2-yl)-5-fluorobenzamide	2D	26	59	29
<i>N</i> -(3-chloro-2-fluorophenyl)-3-cyano-5-fluorobenzamide	2E	8	347	42
<i>N</i> -(3-chloro-4-fluorophenyl)-3-cyano-5-fluorobenzamide	2F	8	377	42
3-cyano- <i>N</i> -(6-methylpyridin-2-yl)benzamide	2G	10	490	29
3-cyano-5-fluoro- <i>N</i> -phenylbenzamide	2H	4	5440	42
<i>N</i> -(adamantan-1-yl)-3-cyano-5-fluorobenzamide	2I	12	>10 000	42
4-aryl-5-cyanopyrimidine (VU0366058) series				
2-(benzo[<i>d</i>]oxazol-2-ylamino)-4-(2-methoxyphenyl)pyrimidine-5-carbonitrile	3A	8	62	26
2-(benzo[<i>d</i>]oxazol-2-ylamino)-4-phenylpyrimidine-5-carbonitrile	3B	8	89	26
2-(benzo[<i>d</i>]oxazol-2-ylamino)-4-(4-fluorophenyl)pyrimidine-5-carbonitrile	3C	8	91	26
2-(benzo[<i>d</i>]oxazol-2-ylamino)-4-cyclohexylpyrimidine-5-carbonitrile	3D	22	216	26
2-(benzo[<i>d</i>]oxazol-2-ylamino)-4-(4-methoxyphenyl)pyrimidine-5-carbonitrile	3E	16	223	26
2-(benzo[<i>d</i>]oxazol-2-ylamino)-4-(3,5-dimethoxyphenyl)pyrimidine-5-carbonitrile	3F	32	>10 000	26
2-(benzo[<i>d</i>]oxazol-2-ylamino)-4-(pyridin-2-yl)pyrimidine-5-carbonitrile	3G	8	>10 000	26
2-(benzo[<i>d</i>]oxazol-2-ylamino)-4-(naphthalen-2-yl)pyrimidine-5-carbonitrile	3H	16	>10 000	26
Aryl ether benzamide NAM (VU0409106) series				
3-chloro-5-((5-fluoropyridin-3-yl)oxy)- <i>N</i> -(6-methylpyridin-2-yl)benzamide	5A	84	5	30
3-chloro- <i>N</i> -(4-methylthiazol-2-yl)-5-(pyrimidin-5-yloxy)benzamide	5B	42	11	30
3-chloro-5-((5-cyanopyridin-3-yl)oxy)- <i>N</i> -(6-methylpyridin-2-yl)benzamide	5C	87	12	30
3-fluoro- <i>N</i> -(4-methylthiazol-2-yl)-5-(pyrimidin-5-yloxy)benzamide	5D	40	26	30
3-chloro- <i>N</i> -(6-methylpyridin-2-yl)-5-(pyrimidin-5-yloxy)benzamide	5E	42	26	30
3-chloro- <i>N</i> -(6-methoxypyridin-2-yl)-5-(pyrimidin-5-yloxy)benzamide	5F	82	49	30
<i>N</i> -(5-fluoropyridin-2-yl)-3-methoxy-5-(pyrimidin-5-yloxy)benzamide	5G	89	85	30
<i>N</i> -(4-methylthiazol-2-yl)-3-(pyrimidin-5-yloxy)benzamide	5H	32	205	30
<i>N</i> -(pyridin-2-yl)-3-(pyridin-3-yloxy)benzamide	5I	84	844	30
3-chloro-5-(pyrimidin-5-yloxy)- <i>N</i> -(5-(trifluoromethyl)pyridin-2-yl)benzamide	5J	38	>10 000	30
3-chloro- <i>N</i> -(3-fluoropyridin-2-yl)-5-(pyrimidin-5-yloxy)benzamide	5K	45	>10 000	30
<i>N</i> -(5-bromo-4-methylthiazol-2-yl)-3-fluoro-5-((2-methylpyrimidin-5-yl)oxy)benzamide	5L	83	>10 000	30

^aStructures for each compound are found in the Supporting Information. ^bNumber of conformers computed for each ligand for docking.

Efforts to develop mGlu₅ allosteric modulators have been particularly successful. Numerous chemotypes have been disclosed that encompass the full range of modulator pharmacology, including weak and full NAMs, ago-PAMs, pure PAMs, and SAMs. Despite this success, structure–activity relationships (SAR) for mGlu modulators are often difficult to interpret. Often, minimal changes to a molecule will translate to a complete loss of activity.⁸ Furthermore, multiple mGlu chemotypes display “molecular switches” where a PAM or SAM arises from a NAM scaffold and vice versa.⁹ These molecular switches have been noted in numerous mGlu₅ modulator chemotypes^{10–15} and can also give rise to unanticipated changes in subtype selectivity.¹⁶ This complexity in modulator SAR continues to be a challenge for drug discovery. It is

important to note that the vast majority of discovery programs rely upon potency data alone, such that it remains to be determined whether the “flat” or “steep” SAR and “molecular switches” may be attributed to changes in modulator affinity and/or cooperativity. Thus, there is a pressing need for a better understanding at both the ligand and receptor level as to what contributes to affinity versus cooperativity.

We sought to explore the structural determinants within mGlu₅ required for ligand binding to the common allosteric site, within and across different chemical scaffolds. We employed a suite of single point mutations that are either known or predicted to contribute to the common allosteric site.^{17–23} Six key residues (P654, Y658, T780, W784, S808, and A809) were consistently implicated as affinity determinants for

diverse PAMs and NAMs, validating that these seven chemotypes interact with a common binding pocket. However, a number of mutations showed differential effects on affinity and/or cooperativity between different scaffolds. To facilitate interpretation of mutagenic data and delineation of affinity versus cooperativity determinants, 9–10 analogues from each series, including active and inactive compounds, were docked into our comparative model of mGlu₅. Building upon the previous observation that W784 was a crucial for MPEP cooperativity, we found that W784A caused a NAM to PAM switch for two different NAM scaffolds. Herein, we've taken advantage of the plethora of mGlu₅ SAR data to facilitate rationalization of binding pose selection for compounds docked to a mGlu₅ comparative model, strengthening hypotheses regarding the specific ligand–receptor contacts that dictate the binding and cooperativity of diverse allosteric modulators. The results highlight the subtleties of small molecule binding within the mGlu₅ 7TM domain.

RESULTS AND DISCUSSION

Probing Determinants of Allosteric Modulation within the Common Allosteric Site. A common allosteric site of mGlu₅, originally characterized as a site for the mGlu₅ NAM MPEP,^{5,22,24} recognizes multiple chemotypes that encompass the full array of allosteric ligand pharmacology including ago-PAMs, pure PAMs, NAMs, and SAMs.^{3,4,10,13} Developing a deeper understanding of how allosteric ligands occupy the pocket and transmit their cooperativity will be important for interpreting the complexities inherent in allosteric modulator SAR. In addition, these insights will enrich our understanding of how class C GPCRs function and inform drug discovery efforts for this receptor class. To achieve this, we assessed representatives from seven allosteric modulator chemical scaffolds across a panel of single point mutations hypothesized to contribute to a common allosteric site in mGlu₅.^{17–22} Building on our previous findings with MPEP, we assessed M-5MPEP, a related compound with lower affinity and cooperativity, in addition to three full NAMs: VU0285683, VU0366058, and VU0409106; two partial NAMs: VU0366248 and VU0366249; and two PAMs: VU29 and DPFE. Mutations were screened for the effect of a single, submaximal modulator concentration (based on wildtype) to alter the glutamate concentration response curve for intracellular Ca²⁺ mobilization (Supporting Information Figure 1). Mutations that significantly altered modulation in the single concentration screen (Supporting Information Figure 2) were assessed using the operational model of allosterism to determine modulator affinity and cooperativity estimates.²⁵ As expected for ligands interacting with a common pocket, many similarities were seen with respect to the impact of mutations on modulator affinity (Figure 1).

Identification of NAM–Receptor Interactions That Govern Affinity. With few exceptions, P654, Y658, T780, W784, S808, and A809 were implicated as affinity determinants, in good agreement with previous studies.^{18–22} To facilitate interpretation of mutagenesis data, representatives from each NAM chemotype (VU0366248, VU0409106, VU0285683, VU0366058) were docked into our comparative model of the mGlu₅ 7TM domains in comparison with the reference prototypical NAM, MPEP.¹⁷ In our previous efforts investigating the binding modes of MPEP and acetylenic PAMs, we found it difficult to computationally differentiate binding poses of these relatively linear ligands.¹⁷ Therefore, we took

advantage of the wealth of available SAR data for these different chemotypes to strengthen interpretations of putative binding poses with the aim to define the specific ligand–receptor interactions governing affinity and cooperativity. For mGlu₅ NAMs, with the exception of VU0285683 where very few analogues have been reported,¹² we identified the best-in-class and minimally active pharmacophore for each scaffold (Table 1, Supporting Information Figure 3) and docked 9–12 analogues (Figure 2), including three inactive (or very low potency) compounds. To compare common binding modes across different ligands within the same scaffold, a new measure was introduced called ChargeRMSD. This measure allowed comparison of ligand conformations by their spatial similarity and conservation of chemical properties, such that conserved ligand SAR becomes a key factor to determine binding modes (Supporting Information text and Figure 4). In comparison, traditional RMSD calculations only capture structural similarities between common atoms of ligands.

Direct Interactions with S808 May Mediate Binding of NAMs with Cyano Substitutions on Ring B. All five 4-aryl-5-cyanopyrimidine active ligands converged to two possible binding poses, one with the cyano group buried (Figure 2a), the other with the cyano group pointing toward extracellular space (Figure 2b). The 5-cyano is crucial for potency in this series,²⁶ and if buried within the pocket, a hydrogen bond with T780 is predicted (Figure 2a). However, VU0366058 affinity was unaffected by T780A, favoring the cluster with 5-cyano pointing up (Figure 2b). A cyano group is also a key feature of the *N*-aryl benzamide NAMs (represented by VU0366248); substitution of ring B with 3-cyano yields the most potent ligands.²⁷ We postulate that the cyano group, or possibly the 5-fluoro, interacts with S808 (Figure 2c); consistent with decreased *N*-aryl benzamide (VU0366248 and VU0366249) affinity at S808A while S808T increases affinity. Moreover, T780A had differential effects on the affinity of VU0366248 and VU0366249; these compounds only differ with respect to the position of fluoro substituent on ring A. Interestingly, S808A reduced M-5MPEP affinity by 260 fold versus only 40 fold for MPEP. We previously hypothesized that S808 may be crucial for initial receptor recognition by MPEP via the pyridine ring. Indeed, the position of the nitrogen in the pyridine ring is crucial for NAM activity.²⁸ Docking of acetylene NAMs with methoxy substituents (1C, 1F, 1G) on ring B (Figure 2g) revealed the methoxy groups coordinated in close proximity to S808. Thus, the increased sensitivity of M-5MPEP to S808A may be related to the 2-methoxy group and/or the pyridine ring interacting with S808. Furthermore, docking of the subnanomolar potency analog (1A) that contains a cyano substitution on ring B suggested a potential hydrogen bond with S808 (Figure 2h). Inactive compounds in both the 4-aryl-5-cyanopyrimidine and *N*-aryl benzamide series docked with the cyano group buried in the pocket (Supporting Information Figure 5). VU0366058 and VU0285683 cooperativity was reduced at S808T and S808A, where these compounds could no longer abolish glutamate activity; however, MPEP and VU0409106 retained full blockade (Table 3). Conversely, VU0366248 and VU0366249, both weak (or partial) NAMs at the wildtype receptor, fully blocked glutamate activation of S808T, suggestive of increased negative cooperativity. Importantly, all four NAMs that show altered cooperativity contain a cyano group. These data lend additional support to diverse NAMs binding with ring B higher in the pocket and, where present, a cyano group directly interacting with S808.

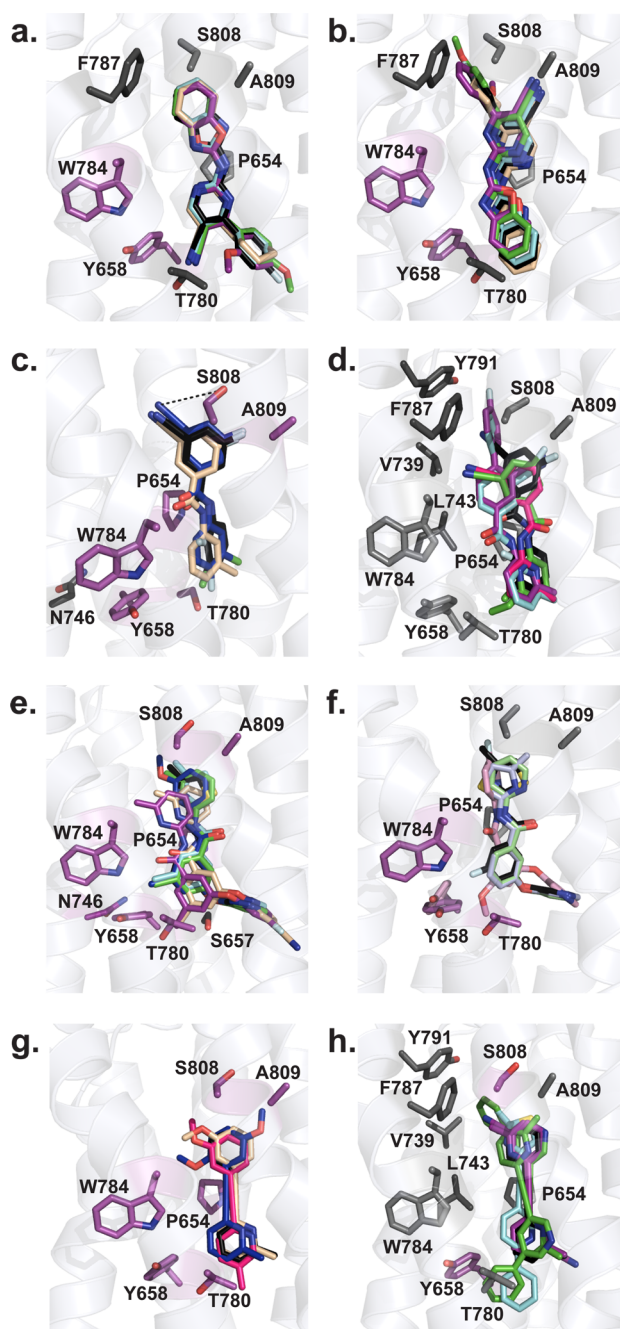


Figure 2. Combining mutagenesis and SAR to understand binding modes of mGlu₃ NAMs. Binding modes from the largest clusters for each ligand are shown, docked into the mGlu₃ comparative model. Key residues implicated in ligand affinity for each scaffold, in addition to the six residues (P654, Y658, T780, W784, S808, and A809) identified as key determinants across all seven scaffolds, are shown in sticks. (a, b) 4-Aryl-5-cyanopyrimidine NAM docking with 3A in purple, 3B in cyan, 3C (VU0366058) in black, 3D in beige, and 3E in green. (c, d) Docking of *N*-aryl benzamide NAMs with 2A in purple, 2B in cyan, 2C in beige, 2D in green, 2E (VU0366248) in black, 2F in blue, and 2G in pink. (e, f) Docking of aryl ether benzamide NAMs with 5A in purple, 5B in cyan, 5C in beige, 5D (VU0409106) in black, 5E in green, 5F in blue, 5G in light pink, 5H in light blue, and 5I in light green. (g, h) Acetylene NAM docking with 1A in purple, 1B in cyan, 1C in beige, 1D in green, 1E (MPEP) in black, 1F in blue, and 1G in pink.

Hydrophobic Residue Cluster in TM5/6 May Limit Substitution on Ring B of NAMs. The most potent/highest

affinity *N*-aryl benzamides, for example, 2A and 2B, have an additional phenyl substitution on ring B.²⁹ Examination of the putative binding pose reveals engagement of cluster of hydrophobic residues in TMS and 6 (V739, L743, F787, and Y791) and potentially a polar interaction between the 4-fluoro of 2A and Y791. The result is a markedly different binding mode compared to reference compound VU0366248 (Figure 2d); whereas analogues with a pyridine ring A (2D and 2G) align closer to the VU0366248 cluster. Furthermore, F787A and Y791A increased VU0366058 affinity by 13- and ~2.6-fold, respectively (Y791A in Supporting Information table); this may be attributed to removal of steric constraints freeing up space in the pocket to accommodate the fluoro-phenyl substituent. These data lend even further support for the putative binding mode with 5-cyano pointing up (Figure 2b). Bulky substitutions of this phenyl and polar substitutions were not well tolerated;²⁶ inactive compounds in the aryl ether NAM series introduce bulk (e.g., 5L) or polarity (e.g., 5J and 5K) onto ring B (Supporting Information Figure 5).³⁰ Furthermore, analogues of MPEP with a phenyl substitution on ring B (e.g., 1D in Figure 2h) may engage with this hydrophobic cluster; although if ring B is buried, π - π stacking may occur between Y658 and the ligand. Docking of inactive MPEP analogues (Supporting Information Figure 5) revealed that substantial reorientation of binding pocket residues was required to accommodate the large substitutions of ring B (F787 for 1I and R647 for 1J). Collectively, these data are commensurate with the cluster of hydrophobic residues in TMS/6 having the potential to contribute to high affinity binding, but also limiting the size and polar nature of substitution on ring B of NAMs.

Surprisingly, the O-linked heteroaryl group of the aryl ether benzamide NAMs docked deeper into the binding pocket, rather than interacting with the TMS/6 hydrophobic cluster. This binding pose is favored due to multiple polar interactions predicted between the pyrimidine and backbone of TM7 residues and S657 and T780 side chains (Figure 2e). From the single concentration screen, S657A and S657C had no effect on modulation by VU0409106 (Supporting Information Figure 5); however, T780A reduced affinity ~10-fold. These data suggest that interactions with T780 and possibly TM7 are more crucial for high affinity binding of VU0409106 and analogues thereof. Further, for the most potent compounds in this series, chloro or fluoro substituents on benzamide ring A are located in the base of the pocket surrounded by W784, T780, and Y658, commensurate with the impact of mutations on VU0409106 affinity (Figure 1). The minimally active compounds (5H and 5I) lack a substituent in this position, which may account for their drop in potency; whereas methoxy substitution (5G) requires movement of Y658 to occupy the same relative pocket (Figure 2f).

Amide Containing NAMs Are Sensitive to N746A. Interestingly, N746A significantly reduced *N*-aryl benzamide affinity (20-fold for VU0366248 and greater than 10-fold for VU0366249) and VU0409106 affinity (15-fold). Reduced affinity was also observed for VU0285683 (~5-fold), although this did not reach significance. No direct interactions are predicted between these four NAMs and N746. Thus, these effects may be due to indirect changes in the pocket conformation that amide-containing ligands (or those with an oxadiazole replacement) are more sensitive to; such that N746 is important for the overall structure of the binding pocket rather than forming a direct ligand contact.

Table 2. Structure–Activity Relationships of mGlu₅ Positive Allosteric Modulators from Two Diverse Scaffolds Chosen for This Study^a

allosteric ligand	ID	Conf ^b	EC ₅₀ (nM)	ref
<i>N</i> -aryl piperazine (DPFE) series				
1-(4-(2,4-difluorophenyl)piperazin-1-yl)-2-((4-fluorobenzyl)oxy)ethanone	6A	144	100	31
5-((2-(4-(2,4-dichlorophenyl)piperazin-1-yl)-2-oxoethoxy)methyl)thiophene-2-carbonitrile	6B	275	210	33
2-(4-(2-(benzyloxy)acetyl)piperazin-1-yl)benzotrile	6C	146	320	15
1-(4-(2,4-dichlorophenyl)piperazin-1-yl)-4-(pyridin-4-yl)butan-1-one	6D	151	530	33
2-(benzylthio)-1-(4-(2,4-dichlorophenyl)piperazin-1-yl)ethanone	6E	156	710	33
1-(4-(2,4-dichlorophenyl)piperazin-1-yl)-2-((pyridin-4-ylmethyl)amino)ethanone	6F	170	850	33
1-(2-(benzyloxy)ethyl)-4-(2,4-dichlorophenyl)piperazine	6G	410	>25 000	33
1-(4-(2-chloro-4-fluorophenyl)piperidin-1-yl)-2-(pyridin-4-ylmethoxy)ethanethione	6H	131	>10 000	33
2-(4-(2-(cyclopentylmethoxy)acetyl)piperazin-1-yl)benzotrile	6I	449	>10 000	^c
diphenylpyrazolebenzamide (VU29) series				
<i>N</i> -(1,3-diphenyl-1 <i>H</i> -pyrazol-5-yl)-4-nitrobenzamide	4A	7	9	34
<i>N</i> -(1,3-diphenyl-1 <i>H</i> -pyrazol-5-yl)-3,4-dimethylbenzamide	4B	13	17	34
3-cyano- <i>N</i> -(1,3-diphenyl-1 <i>H</i> -pyrazol-5-yl)benzamide	4C	16	45–77	34
<i>N</i> -(1,3-diphenyl-1 <i>H</i> -pyrazol-5-yl)-3-nitrobenzamide	4D	15	39	34
(<i>E</i>)-4-cyano- <i>N</i> -(1-(4-cyanobenzoyl)-2,5-diphenyl-1 <i>H</i> -pyrazol-3(2 <i>H</i>)-ylidene)benzamide	4E	8	43	35
<i>N</i> -(1,3-diphenyl-1 <i>H</i> -pyrazol-5-yl)-4-methoxybenzamide	4F	14	54	35
<i>N</i> -(1,3-diphenyl-1 <i>H</i> -pyrazol-5-yl)benzamide	4G	5	175	34
<i>N</i> -(3-phenyl-1-(pyridin-2-yl)-1 <i>H</i> -pyrazol-5-yl)benzamide	4H	2	>10 000	35
<i>N</i> -(1,3-diphenyl-1 <i>H</i> -pyrazol-5-yl)cyclopentanecarboxamide	4I	15	3410	35
<i>N</i> -(1,3-diphenyl-1 <i>H</i> -pyrazol-5-yl)-3,4-dimethoxybenzamide	4J	87	3530	35

^aStructures for each compound are found in the Supporting Information. ^bNumber of conformers sampled for ligand docking. ^cUnpublished observation from ref 15; synthesis reported in the Supporting Information.

Table 3. Summary of Qualitative and Quantitative Cooperativity Estimates (log β) for mGlu₅ NAMs at Mutant Constructs^a

mutant	M-5MPEP	VU0366058	VU0285683	VU0409106	VU0366248	VU0366249
R5-wt	−1.00 ± 0.11	Full NAM	Full NAM	Full NAM	−0.88 ± 0.11	−0.66 ± 0.18
P654F	Weak NAM	No NAM	No NAM	No NAM	No NAM	No NAM
P654S	−0.37 ± 0.08^b	−0.45 ± 0.08	Full NAM	Full NAM	−0.30 ± 0.09^b	Weak NAM
S657C	Full NAM	n.d.	n.d.	n.d.	Full NAM	−0.23 ± 0.07
S657A	Full NAM	n.d.	n.d.	n.d.	Full NAM	Full NAM
Y658V	Weak NAM	−0.36^c	Full NAM	−0.75 ± 0.10	Full NAM	No NAM
P742S	Full NAM	n.d.	Full NAM	n.d.	n.d.	No NAM
N746A	Full NAM	−0.39 ± 0.15	Full NAM	Full NAM	−1.20 ± 0.08	Weak NAM
G747V	−0.46 ± 0.18	Full NAM	Full NAM	Full NAM	Full NAM	Full NAM
T780A	−0.56 ± 0.08	−0.55 ± 0.06	Full NAM	−0.82 ± 0.09	Full NAM	Weak NAM
W784A	No NAM	−0.50 ± 0.17	0.27 ± 0.06	−0.43 ± 0.08	0.29 ± 0.05^b	0.36 ± 0.06^b
F787A	Full NAM	Full NAM	Full NAM	Full NAM	No NAM	No NAM
V788A	−0.72 ± 0.22	Full NAM	Full NAM	Full NAM	Full NAM	Full NAM
F792A	n.d.	n.d.	n.d.	Full NAM	Full NAM	n.d.
S808A	−0.66 ± 0.11	−0.44 ± 0.10	−0.59 ± 0.14	Full NAM	−0.80 ± 0.35	No NAM
S808T	−0.55 ± 0.19	−0.39 ± 0.09	−0.77 ± 0.19	Full NAM	Full NAM	Full NAM
A809V	Full NAM	Full NAM	Full NAM	Full NAM	Full NAM	No NAM
A809G	−0.43^c	−0.52 ± 0.10	Full NAM	Full NAM	−0.48 ± 0.07	No NAM

^aData are mean ± SEM of 3–5 independent experiments, unless noted otherwise. “Weak NAM” denotes incomplete and nonsaturating inhibition of the glutamate response. “Full NAM” denotes complete abolishment of the glutamate Ca²⁺ mobilization response. “No NAM” indicates no inhibition of the glutamate response was observed up to 10 μM. n.d. denotes not determined. Mutations of the six common determinant residues are highlighted in bold text. ^bSignificantly different to wild type, one-way ANOVA, *p* < 0.05 Dunnett’s post-test. ^cData are mean from two independent experiments.

Determinants of *N*-Aryl Piperazine PAM Binding.

Previously we had examined the interactions of acetylenic PAMs within the common allosteric site of mGlu₅,¹⁷ it was of interest whether PAMs from alternate scaffolds would share affinity and cooperativity determinants. On the whole, the *N*-aryl piperazines are low affinity, cooperativity driven PAMs. Despite this limitation, three compounds from this series are efficacious *in vivo*.^{15,31,32} Consistent with interactions within the common allosteric site, P654S, Y658V, T780A, W784A,

A809G, and A809V decreased affinity of DPFE (6–70-fold). In contrast to all other modulators tested to date, DPFE was unaffected by P654F (Figure 3a). This may be attributable to increased flexibility of this compound allowing binding despite the introduction of a bulky hydrophobic group. Docking results suggest a conserved and relatively linear binding mode, with ring C oriented to the top of the pocket in the vicinity of the TMS/6 hydrophobic cluster and ring A buried; the carbonyl linker may participate in hydrogen bonds with TM7 residues

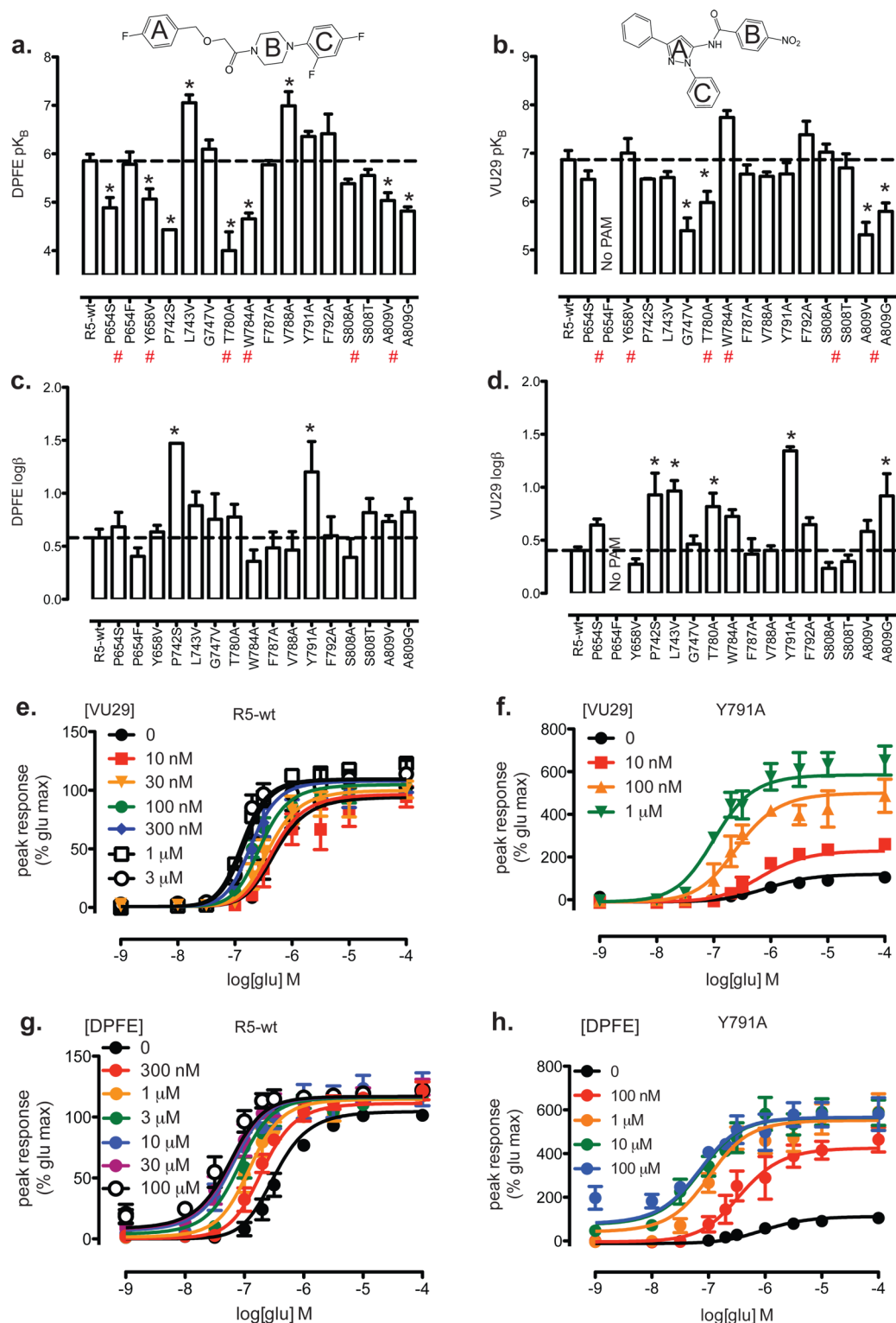


Figure 3. Impact of mutations within the common allosteric site on mGlu₃ PAMs. Progressive modulator-induced shifts in the glutamate concentration response curve for calcium mobilization were quantified with the operational model of allosterism to estimate affinity for (a) VU29 and (b) DPFE as well as cooperativity for (c) DPFE and (d) VU29. VU29 potentiation of glutamate-mediated Ca²⁺ mobilization at wild-type (e) and Y791A (f). DPFE potentiation of glutamate-mediated Ca²⁺ mobilization at wild-type (g) and Y791A (h). Data represent mean ± s.e.m of a minimum of three independent experiments, unless indicated otherwise (Supporting Information table). * indicates significantly different to wild type value, *p* < 0.05, one-way ANOVA with Dunnett's post-test. # denotes key determinant residue identified from mutagenesis.

(Figure 3a). The cyano groups at opposite ends of compounds 6B and 6C are in close proximity to T780 and S808 respectively. In support of this binding mode, we found that compound 6B (VU0364289) was sensitive to the S808A

mutation (Supporting Information Figure 7). This pose places the fluoro-phenyl of DPFE in close proximity to T780; Ala substitution of this residue had the most marked effect on DPFE affinity (70 fold; Figure 3a). Three additional point

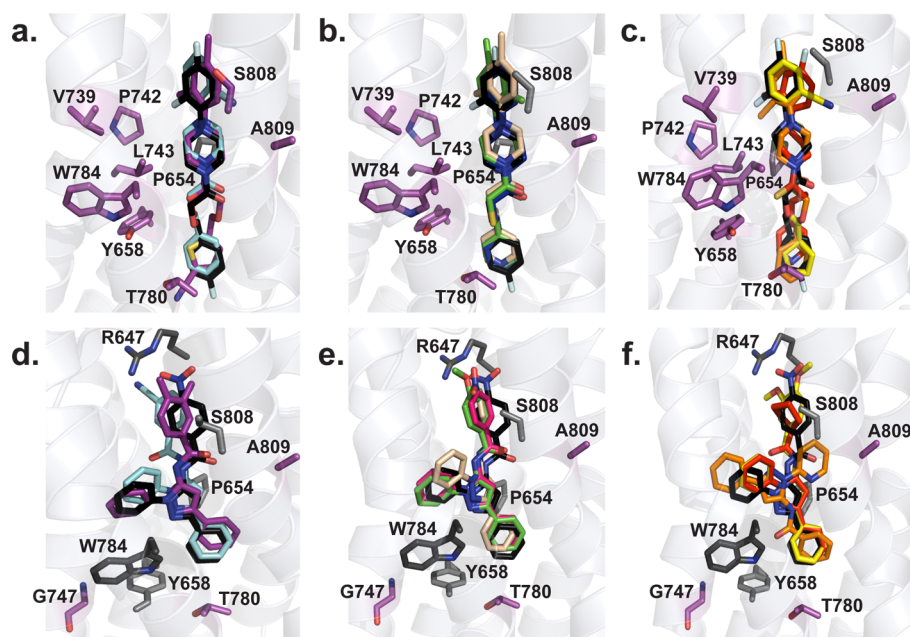


Figure 4. Combining mutagenesis and SAR to understand binding modes of mGlu₅ PAMs. Binding modes from the largest clusters for each ligand are shown highlighting key residues implicated in ligand affinity for each scaffold in addition to the six residues (P654, Y658, T780, W784, S808, and A809) identified as key affinity determinants across all seven allosteric modulator scaffolds. (a–c) Docking of *N*-aryl piperazine PAMs with 6A (DPFE) in black, 6B in purple, 6C in cyan, 6D in beige, 6E in green, 6F in blue, 6G in orange 6H in red, and 6I in yellow. (d–f) Docking of diphenylpyrazole benzamide PAMs with 4A (VU29) in black, 4B in purple, 4C in cyan, 4D in beige, 4F in green, 4G in pink, 4H in orange, 4I in red, and 4J in yellow.

mutations had unique effects on DPFE: P742S decreased affinity (26 fold), L743V increased affinity (16-fold) and V788A increased affinity (14-fold); affinity increases were confirmed with [³H]methoxyPEPy binding assays (Supporting Information Figure 8). Based on the proposed binding mode, these mutations may change the overall binding pocket architecture, in particular, in relation to the TMS/6 hydrophobic cluster and the capacity to accommodate the polar difluorophenyl of DPFE. Minimally active (Figure 4b) and inactive compounds (Figure 4c) in this series adopted a similar pose. In general, inactives lacked a hydrogen bond partner in the linker region to interact with TM7 (e.g., 6G and 6H) or introduced polarity and/or additional bulk to the phenyl ring C that may not be accommodated within the TMS/6 hydrophobic cluster,^{15,33} similar to the observations noted earlier for NAMs.

Affinity Determinants for Diphenylpyrazole Benzamide PAMs. In contrast to all other modulators, VU29 was unaffected by Y658V and compared with other PAMs had a moderate affinity reduction at T780A;¹⁷ possibly due to a lack of hydrogen bond partners in ring A (Figure 3b). This suggests that diphenylpyrazole benzamide PAM activity is driven via interactions higher in the pocket. All diphenylpyrazole benzamide series ligands docked with consistent positions of all three aromatic rings except for 4E (Figure 4d and e). Notably, ring A of VU29 aligns well with the various NAMs; however, neither ring B nor C overlaps (Figure 6). This deviates significantly from that proposed previously based on 3D superimposition of related ligands.²⁹ Further, substitution of the benzamide ring (B) is well tolerated,^{29,34,35} with polar interactions predicted between residues at the top of TMS/E2 loop (Figure 4d and e). Moreover, benzamide phenyl replacement with a cyclopentane (4I) or addition of two methoxy groups (4J) significantly lowers PAM potency.³⁶ Furthermore, docking of inactive compounds showed deviation

from actives, for example, phenyl ring C replacement with a pyridine that abolishes PAM activity (4H; Figure 4f). Indeed, pyridyl replacement or substitution of this phenyl is not tolerated.³⁵ G747V selectively reduced VU29 affinity (30-fold); therefore, we assessed the ability of VU29 to inhibit [³H]methoxyPEPy binding at G747V (Supporting Information Figure 8). VU29 behaved noncompetitively, unable to fully displace [³H]methoxyPEPy binding; recent disclosure of potent dimeric MPEP analogs also suggested the common allosteric pocket could accommodate two ligands simultaneously.^{20,37} Collectively, these data support a global conformation change in the allosteric site architecture in G747V mutation particularly with respect to TMS/6 hydrophobic residues that may interact with ring C (Figure 4e). This is an area of the binding pocket that the other modulators tested do not extend into, therefore accounting for the selective effect of this residue on VU29.

W784 Is a NAM Cooperativity Determinant and Can Engender a “Molecular Switch” to PAM. Similar to its effect on MPEP,¹⁷ W784A reduced cooperativity of the full NAMs VU0366058 and VU0409106 and abolished M-5MPEP cooperativity and/or affinity (Table 3). Interestingly allosteric modulators VU0285683, VU0366248, and VU0366249 which all maintain a common 3-cyano-5-fluoro pendant phenyl ring, switched their pharmacology to PAMs (Figure 5). These data beg the question: What is different about how the W784A receptor interacts with VU0366248 and VU0285683 that allows this dramatic switch? W784 is equivalent to Trp of the CWxP motif in class A 7TMRs that is involved in receptor activation.³⁸ Small increases in positive cooperativity of some, but not all, acetylene PAMs were noted at W784A previously^{17,23} while VU29 and DPFE cooperativities were unaffected (Figure 3c and d) by W784A. Importantly, this mutation does not increase the efficacy of glutamate,¹⁷ nor do NAMs show inverse agonism indicative of constitutive activity. This differential effect of

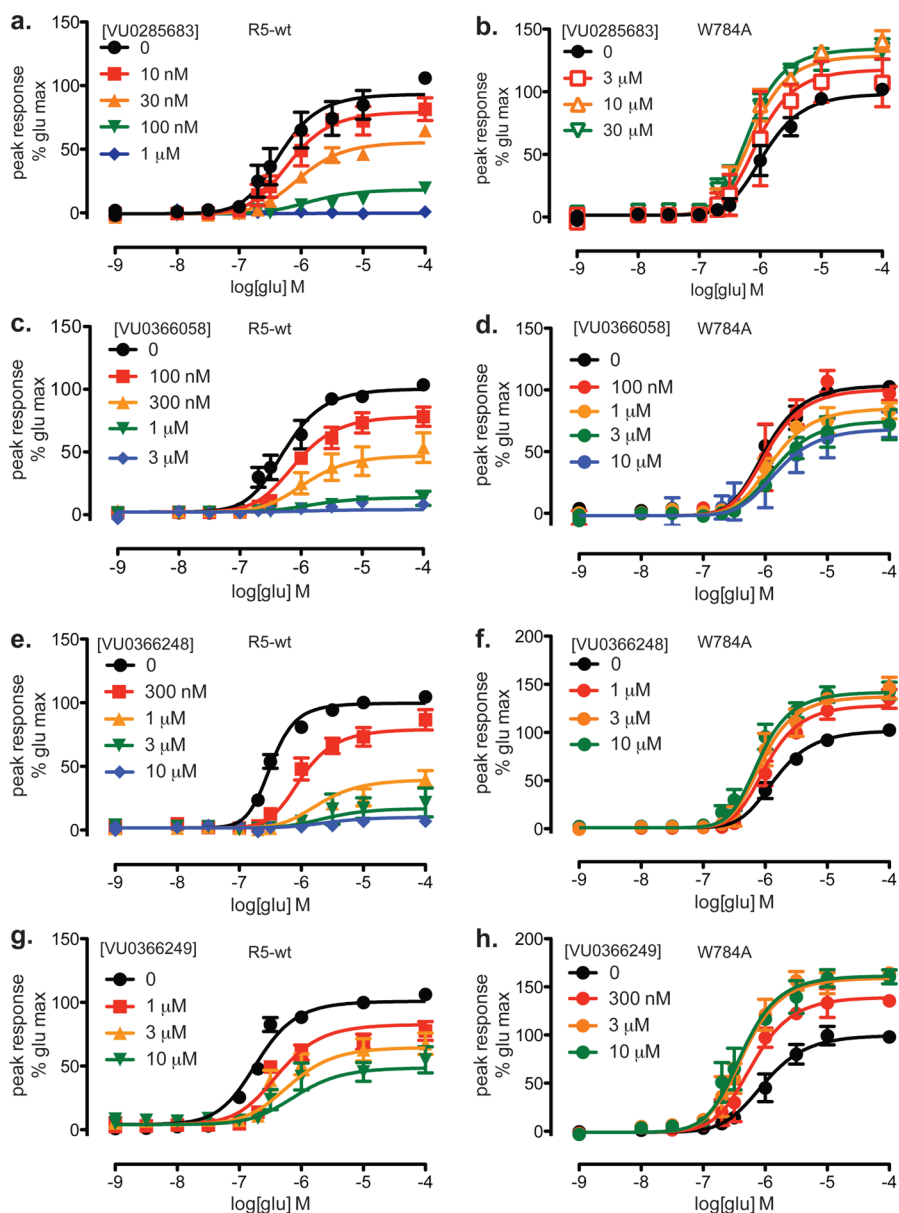


Figure 5. W784A impacts NAM cooperativity and can cause a molecular switch from NAM to PAM. Glutamate-mediated Ca^{2+} mobilization is inhibited by VU0285683 at wild-type (a) and enhanced at W784A (b). VU0366058 completely abolishes glutamate-mediated Ca^{2+} mobilization by at wild-type (c) but has decreased negative cooperativity at W784A (d). Glutamate-mediated Ca^{2+} mobilization is inhibited by VU0366248 and VU0366249 at wild-type (e, g) and enhanced at W784A (f, h). Data represent mean \pm SEM of a minimum of three independent experiments.

W784A on the cooperativity of different NAM and PAM scaffolds is indicative of multiple inactive and active 7TM states being engendered by allosteric modulators, such that this pharmacological mode switch relates to W784A favoring active states that are stabilized by certain modulators. In the case of NAMs VU0366248, VU0366249, and VU0285683 it is conceivable that these modulators have a limited mechanism of action on the molecular level, involving an alternative direct hydrogen bond with W784 with the common cyano moiety that is critical for stabilizing an *inactive* form of the receptor. In the absence of this interaction these modulators elicit moderate positive cooperativity with glutamate (Figure 6, β : ~ 1.9 – 2.3). In contrast, VU0366058 and VU0409106, which do retain similar hydrogen bond accepting groups (e.g., cyano and thiazole, VU0366058 and VU0409106, respectively), may be envisioned as having additional interactions with the receptor

that contribute to the negative cooperativity that is retained at the W784A mutant. Consistent with this notion, VU0366058 and VU0409106 are structurally more complex with a greater number of rotatable bonds (3–4 vs 2 RotB) and hydrogen bond acceptors (6 vs 4); thus, these compounds may be able to adopt multiple positions and/or conformations within the binding pocket to retain their negative cooperativity. In addition, all three weak NAMs (M-5MPEP, VU0366248, and VU0366249) had reduced cooperativity at P654S and increased negative cooperativity at S657A. Together, these data suggest that (1) TM6 and W784, in particular, are crucial for adoption of active receptor states of family C 7TMRs and that (2) these differential effects on cooperativity provide evidence for stabilization of different inactive receptor conformations by individual chemotypes.

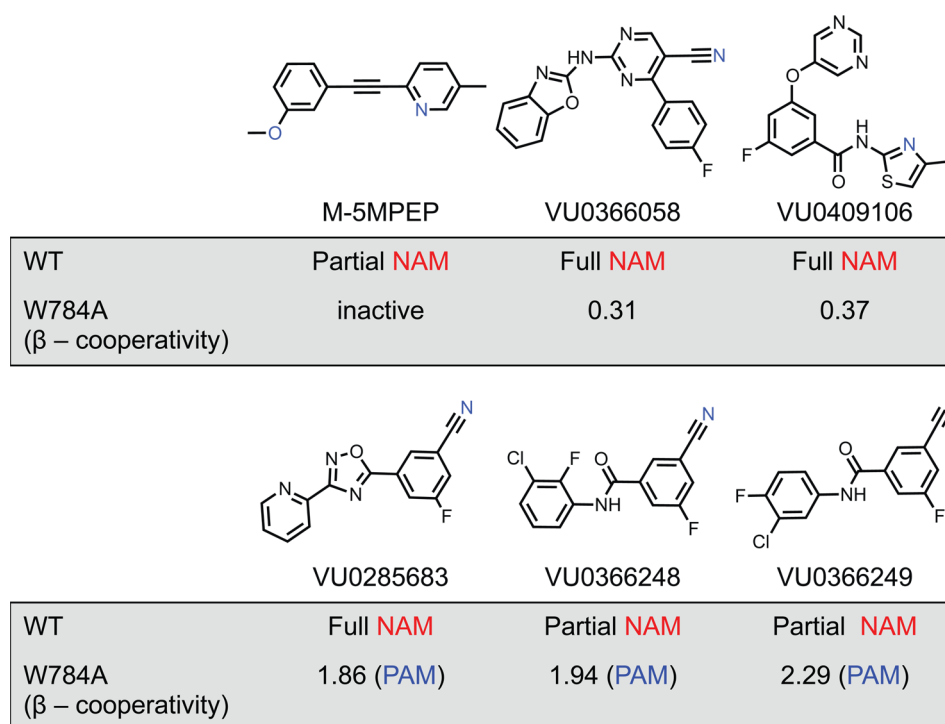


Figure 6. Comparison of modulator scaffolds and relationship to cooperativity at wild-type vs W784A. NAMs in the top panel show reduced negative cooperativity (or are inactive) at W784A. NAMs in the bottom panel that share a common cyano moiety exhibit a mode switch in cooperativity from NAM to PAM at W784A.

PAM Cooperativity Determinants within the Common Allosteric Site. Pharmacological mode switches at T780A, F787A, or S808A have been observed for certain acetylene PAMs and DFB^{17,21,23} and their cooperativity with glutamate; neither VU29 nor DPFE showed mode switches at any of the mutations tested. However, both P742S and Y791A increased positive cooperativity, with increases also noted for VU29 at L743V and T780A (Figure 3c and d). Interestingly, Y791A had very low responsiveness to glutamate prohibiting functional assessment of NAMs; however, this could be restored with PAMs (Figure 3). Collectively, the changes observed for modulator cooperativity highlight the importance of TM3, 5, 6, and 7 in the transmission of cooperativity by both negative and positive mGlu₅ allosteric modulators and infer a role for these TMs in the transition of the 7TM region from inactive to active states.

Docking PAMs into an Inactive Template. An important question in homology modeling 7TMRs in complex with PAMs is whether a 7TMR template in an “active” state must be used. The critical question is this: is there a systematic difference in the position of the upper transmembrane helices between “active” and “inactive” templates that might play a role when docking into such a distant sequence homologue? To answer this question we computed pairwise RMSDs between “active” and “inactive” structures using the structured-based alignment tool MAMMOTH (3.1 ± 0.5 Å RMSD).³⁹ This value is not significantly higher than the average pairwise RMSD between two inactive structures (2.9 ± 0.6) or two active structures (2.8 ± 0.6). We attribute this possibly surprising finding to several aspects: (A) sequence similarity between GPCRs is so low that structural changes induced by a different sequence are larger than structural changes induced by activation, at least in the upper half of the trans-membrane spanning regions. (B) One can also argue that many of the “active” conformations might

not be fully active as no G protein was bound. We conclude that there is no advantage in using an “active” template when modeling such distant homologues as the structural changes between template and target will be much larger than changes induced by activation. The Rosetta comparative modeling methods are unique in that the backbone template applied to the comparative model is only used to determine the initial placement in transmembrane helices. In the subsequent energy minimization steps, the backbone template is perturbed on average 6–8 Å RMSD.⁴⁰ In particular, the binding pocket is perturbed on average 2–4 Å RMSD. Additionally, the flexible docking methods are able to capture the different binding modes of active (Figures 2 and 4) versus inactive ligands (Supporting Information Figure 5). In experiments analyzing the accuracy of Rosetta’s ligand docking methods when applied to comparative models, Rosetta sampled ligand binding modes within 2.5 Å of the binding mode from the crystal structure for 14 7TMRs.⁴⁰ In addition to our analysis, Tautermann and Pautsch examined the binding sites of active and inactive β 2-adrenergic receptor.⁴¹ They show that the binding site is very similar between the inactive and active states and conclude that both “active” and “inactive” state structures should be considered as templates.⁴¹ Previous modeling studies with the inactive structure predicted the binding mode of an agonist that overlapped well with that seen in the agonist-bound crystal structure.

Molck and colleagues recently proposed that the binding pocket within the 7TM domains was divided into two by W784, yielding two distinct binding poses for MPEP.²⁰ In our model, employment of flexible docking methodology allows rotation of W784 out of the binding pocket. The binding poses determined by computational docking presented herein were filtered by available SAR and mutagenesis information. This ensures that the final pose selected for each scaffold is within

interaction distance to the residues implicated by mutagenesis (Figure 7). Low potency, or inactive, compounds from available

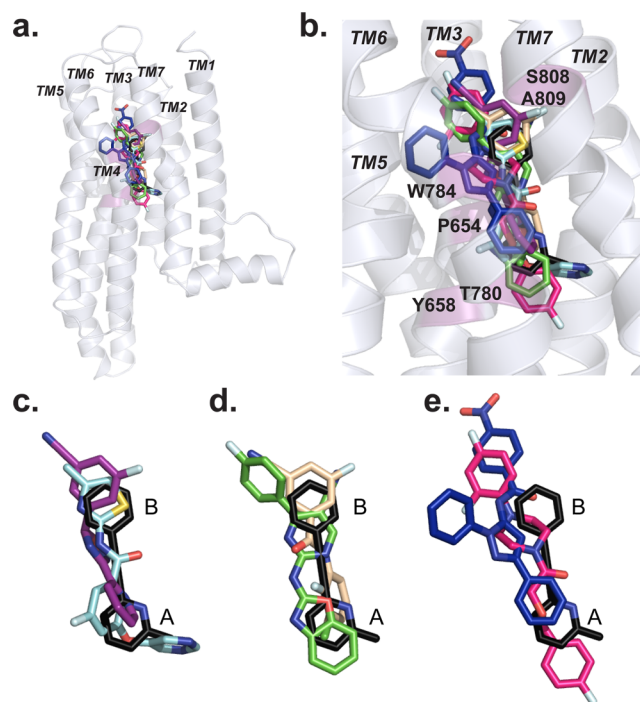


Figure 7. Overlay of top binding modes for diverse allosteric modulator scaffolds. A representative ligand from each scaffold was docked into the mGlu₅ comparative model (a). Binding modes from the largest clusters for each ligand are shown and are within interaction distance of key residues identified from mutational experiments labeled and colored purple (b). Colors corresponding to each ligand are as follows: MPEP is black, VU0285683 is purple, VU0409106 is cyan, VU0366248 is beige, VU0366058 is green, VU29 is blue, and DPFE is pink. Positions of aromatic rings “A” and “B” are similar in (c) MPEP, VU0285683, and VU0409106 as well as (d) MPEP, VU0366248, and VU0366058. (e) While ring position is not conserved, linear positioning of MPEP, VU29, and DPFE is similar when interacting with the common allosteric site.

SAR were selected that retain some activity to avoid the potential confound of neutral allosteric ligands, that is, allosteric ligands that occupy the binding pocket but do not modulate receptor activity. Thus, these “inactive” ligands were assumed to be the result of low compatibility with the binding pocket. It is conceivable that inactive compounds may be the result of simply being unable to enter the binding pocket. Currently, for family C 7TMRs, there is a lack of appreciation of how allosteric modulators access the transmembrane domains. Lipophilic compounds may enter the pocket via the lipid bilayer or from the top of the pocket opening to extracellular space. In the absence of a family C 7TMR crystal structure, these models are not expected to provide high-resolution predictions. However, coupling of mutagenesis-based studies with comparative modeling of 7TMRs has provided powerful tools to study drug–receptor interactions for receptors where crystal structures are unavailable. We anticipate that employment of such a strategy would be operative at other receptors where crystal structures are not available. By applying an operational model of allostery to quantify the impact of mutations on modulator pharmacology we have learnt further power to these analyses, differentiating between effects on

affinity versus cooperativity. We identified a single point mutation (W784A) that engendered a molecular switch in NAM pharmacology for two different scaffolds, providing additional insight from the protein perspective as to the propensity of mGlu₅ modulator SAR to display molecular switches. It is apparent that a deeper understanding of the specific ligand–receptor interactions has the potential to inform modulator design and potentially aid drug discovery efforts for this important CNS target.

METHODS

Materials. Dulbecco’s modified Eagle’s medium (DMEM), fetal bovine serum (FBS), and antibiotics were purchased from Invitrogen (Carlsbad, CA). VU0409106, VU0366058, VU0366248, VU0366249, M-SMPEP, VU29, DPFE, and analogues thereof were all synthesized in-house using previously reported methodologies.^{13,15,26,30,31,34,42} Synthesis of compound 6I is reported in the Supporting Information. Unless otherwise stated, all other reagents were purchased from Sigma-Aldrich (St. Louis, MO) and were of an analytical grade.

Cell Culture. Mutations were introduced into the wild type rat mGlu₅ as described previously.¹⁷ Polyclonal stable HEK293A-mGlu₅ mutant cell lines were maintained in complete DMEM supplemented with 10% FBS, 2 mM L-glutamine, 20 mM HEPES, 0.1 mM non-essential amino acids, 1 mM sodium pyruvate, antibiotic–antimycotic, and 500 μg/mL G418 at 37 °C in a humidified incubator containing 5% CO₂, 95% O₂.

Intracellular Ca²⁺ Mobilization. Prior to assay, HEK293A-rat mGlu₅ cells were seeded at 50 000 cells/well in poly-D-lysine coated black-walled, clear bottom 96-well plates in assay medium (DMEM with 10% dialyzed FBS, 20 mM HEPES, 1 mM sodium pyruvate). On the day of assay, the cell permeable Ca²⁺ indicator dye Fluo-4 (Invitrogen, Carlsbad, CA) was used to assay receptor-mediated Ca²⁺ mobilization as described previously^{17,25} using a Flexstation II (Molecular Devices, Sunnyvale, CA) instrument.

Docking Allosteric Modulators into the mGlu₅ Comparative Model. A total of 60 ligands were chosen for computational ligand docking (Tables 1 and 2). Conformers for each ligand were first generated with MOE (Molecular Operating Environment, Chemical Computing Group, Ontario, Canada) using the MMFF94x force field and Generalized Born implicit solvent model. Ligand conformers were generated, dependent on the number of rotatable bonds (Table 1), using 10 000 iterations of the Low Mode MD method⁴³ with a redundancy cutoff of 0.25 Å. Ligands were then computationally docked into our comparative model of mGlu₅¹⁷ using Rosetta Ligand.^{44–46} Three rounds of iterative docking were performed, and analysis within and across different scaffolds was based on a new measure called ChargeRMSD (see the Supporting Information for further details).

ASSOCIATED CONTENT

Supporting Information

General chemistry methods for previously unpublished compounds, additional detail for docking of allosteric modulators and the new clustering method used, as well as additional functional and binding data sets to support the conclusions in the text. This material is available free of charge via the Internet at <http://pubs.acs.org>.

AUTHOR INFORMATION

Corresponding Authors

*E-mail: jens.meiler@vanderbilt.edu.

*E-mail: jeff.conn@vanderbilt.edu.

Author Contributions

▽K.J.G. and E.D.N. contributed equally to this work. K.J.G., E.D.N., C.M., J.M. and P.J.C. conceived and designed the experiments. K.J.G., E.D.N., C.M., J.L.M., J.Z.Z., B.S.B., M.J.N.,

E.F.S., E.M.T., J.M.R., K.A.E. and S.R.S. performed the experiments and analyzed the data. K.J.G., E.D.N., C.M. and S.R.S. interpreted the data and prepared the figures. J.L.M., K.A.E., S.R.S. and C.W.L. contributed materials, reagents and analysis tools. K.J.G., E.D.N., S.R.S., J.M. and P.J.C. wrote the manuscript.

Funding

This work is supported by the National Institute of Mental Health [Grant 2R01 MH062646-13]; National Institute of Neurological Disorders and Stroke (NINDS) [Grant 2R01 NS031373-16A2]; National Institute of Drug Abuse [Grant 1R01 DA023947]; and Molecular Libraries Probe Production Centers Network [Grant 5 u54 MH84659-03, 5 u54 MH84659-03S1]. K.J.G. is the recipient of: National Alliance for Research on Schizophrenia and Depression-Maltz Young Investigator Award; American Australian Association Merck Foundation Fellowship; and National Health and Medical Research Council (Australia) Overseas Biomedical Postdoctoral Training Fellowship. E.D.N. is funded by the PhRMA Foundation Paul Calabresi Medical Student Fellowship. M.J.N. is supported by a National Research Service Award from NINDS [Grant F32 NS071746]. Work in the Meiler laboratory is supported through the National Institutes of Health [R01 GM080403, R01 MH090192, R01 GM099842] and the National Science Foundation [Career 0742762].

Notes

The authors declare the following competing financial interest(s): Over the past two years, Dr. Conn has served as a consultant for Millipore Corp. (St. Charles, Missouri) and on the Scientific Advisory Board of Seaside Therapeutics (Boston, Massachusetts) and Karuna Pharmaceuticals (Boston, Massachusetts). Dr. Conn has received research funding from Janssen Pharmaceutica (Beerse, Belgium) and Seaside Therapeutics (Boston, Massachusetts) and is engaged in collaborations with both companies that have the potential of generating milestone and royalty payments. Dr. Conn, Dr. Lindsley, Dr. Emmitte, and Dr. Stauffer receive/d salary support from Johnson and Johnson and/or Seaside Therapeutics. Dr. Conn, Dr. Lindsley, Dr. Stauffer, and Dr. Emmitte are inventors on multiple pending and issued patents that protect different classes of allosteric modulators of mGlu5 and other GPCRs.

ACKNOWLEDGMENTS

The authors acknowledge Philine Hietschold for her contribution to initial docking studies.

REFERENCES

- (1) Niswender, C. M., and Conn, P. J. (2010) Metabotropic glutamate receptors: physiology, pharmacology, and disease. *Annu. Rev. Pharmacol. Toxicol.* 50, 295–322.
- (2) Gregory, K. J., Noetzel, M. J., and Niswender, C. M. (2013) Pharmacology of metabotropic glutamate receptor allosteric modulators: structural basis and therapeutic potential for CNS disorders. *Prog. Mol. Biol. Transl. Sci.* 115, 61–121.
- (3) Stauffer, S. R. (2011) Progress toward Positive Allosteric Modulators of the Metabotropic Glutamate Receptor Subtype 5 (mGlu5). *ACS Chem. Neurosci.* 2, 450–470.
- (4) Emmitte, K. A. (2011) Recent Advances in the Design and Development of Novel Negative Allosteric Modulators of mGlu5. *ACS Chem. Neurosci.* 2, 411–432.
- (5) Gasparini, F., Lingenhohl, K., Stoehr, N., Flor, P. J., Heinrich, M., Vranesic, I., Biollaz, M., Allgeier, H., Heckendorn, R., Urwyler, S., Varney, M. A., Johnson, E. C., Hess, S. D., Rao, S. P., Sacca, A. I., Santori, E. M., Velicelbi, G., and Kuhn, R. (1999) 2-Methyl-6-

(phenylethynyl)-pyridine (MPEP), a potent, selective and systemically active mGlu5 receptor antagonist. *Neuropharmacology* 38, 1493–1503.

- (6) Varney, M. A., Cosford, N. D., Jachec, C., Rao, S. P., Sacca, A., Lin, F. F., Bleicher, L., Santori, E. M., Flor, P. J., Allgeier, H., Gasparini, F., Kuhn, R., Hess, S. D., Velicelbi, G., and Johnson, E. C. (1999) SIB-1757 and SIB-1893: selective, noncompetitive antagonists of metabotropic glutamate receptor type 5. *J. Pharmacol. Exp. Ther.* 290, 170–181.

- (7) Noetzel, M. J., Rook, J. M., Vinson, P. N., Cho, H. P., Days, E., Zhou, Y., Rodriguez, A. L., Lavreysen, H., Stauffer, S. R., Niswender, C. M., Xiang, Z., Daniels, J. S., Jones, C. K., Lindsley, C. W., Weaver, C. D., and Conn, P. J. (2012) Functional impact of allosteric agonist activity of selective positive allosteric modulators of metabotropic glutamate receptor subtype 5 in regulating central nervous system function. *Mol. Pharmacol.* 81, 120–133.

- (8) Zhao, Z., Wisnoski, D. D., O'Brien, J. A., Lemaire, W., Williams, D. L., Jr., Jacobson, M. A., Wittman, M., Ha, S. N., Schaffhauser, H., Sur, C., Pettibone, D. J., Duggan, M. E., Conn, P. J., Hartman, G. D., and Lindsley, C. W. (2007) Challenges in the development of mGluR5 positive allosteric modulators: the discovery of CPPHA. *Bioorg. Med. Chem. Lett.* 17, 1386–1391.

- (9) Wood, M. R., Hopkins, C. R., Brogan, J. T., Conn, P. J., and Lindsley, C. W. (2011) "Molecular switches" on mGluR allosteric ligands that modulate modes of pharmacology. *Biochemistry* 50, 2403–2410.

- (10) Hammond, A. S., Rodriguez, A. L., Townsend, S. D., Niswender, C. M., Gregory, K. J., Lindsley, C. W., and Conn, P. J. (2010) Discovery of a Novel Chemical Class of mGlu(5) Allosteric Ligands with Distinct Modes of Pharmacology. *ACS Chem. Neurosci.* 1, 702–716.

- (11) Lamb, J. P., Engers, D. W., Niswender, C. M., Rodriguez, A. L., Venable, D. F., Conn, P. J., and Lindsley, C. W. (2011) Discovery of molecular switches within the ADX-47273 mGlu5 PAM scaffold that modulate modes of pharmacology to afford potent mGlu5 NAMs, PAMs and partial antagonists. *Bioorg. Med. Chem. Lett.* 21, 2711–2714.

- (12) Rodriguez, A. L., Grier, M. D., Jones, C. K., Herman, E. J., Kane, A. S., Smith, R. L., Williams, R., Zhou, Y., Marlo, J. E., Days, E. L., Blatt, T. N., Jadhav, S., Menon, U. N., Vinson, P. N., Rook, J. M., Stauffer, S. R., Niswender, C. M., Lindsley, C. W., Weaver, C. D., and Conn, P. J. (2010) Discovery of novel allosteric modulators of metabotropic glutamate receptor subtype 5 reveals chemical and functional diversity and in vivo activity in rat behavioral models of anxiolytic and antipsychotic activity. *Mol. Pharmacol.* 78, 1105–1123.

- (13) Rodriguez, A. L., Nong, Y., Sekaran, N. K., Alagille, D., Tamagnan, G. D., and Conn, P. J. (2005) A close structural analog of 2-methyl-6-(phenylethynyl)-pyridine acts as a neutral allosteric site ligand on metabotropic glutamate receptor subtype 5 and blocks the effects of multiple allosteric modulators. *Mol. Pharmacol.* 68, 1793–1802.

- (14) Sharma, S., Kedrowski, J., Rook, J. M., Smith, R. L., Jones, C. K., Rodriguez, A. L., Conn, P. J., and Lindsley, C. W. (2009) Discovery of molecular switches that modulate modes of metabotropic glutamate receptor subtype 5 (mGlu5) pharmacology in vitro and in vivo within a series of functionalized, regioisomeric 2- and 5-(phenylethynyl)-pyrimidines. *J. Med. Chem.* 52, 4103–4106.

- (15) Zhou, Y., Manka, J. T., Rodriguez, A. L., Weaver, C. D., Days, E. L., Vinson, P. N., Jadhav, S., Hermann, E. J., Jones, C. K., Conn, P. J., Lindsley, C. W., and Stauffer, S. R. (2010) Discovery of N-Aryl Piperazines as Selective mGluR5 Potentiators with Improved In Vivo Utility. *ACS Med. Chem. Lett.* 1, 433–438.

- (16) Sheffler, D. J., Wenthur, C. J., Bruner, J. A., Carrington, S. J. S., Vinson, P. N., Gogi, K. K., Blobaum, A. L., Morrison, R. D., Vamos, M., Cosford, N. D. P., Stauffer, S. R., Scott Daniels, J., Niswender, C. M., Jeffrey Conn, P., and Lindsley, C. W. (2012) Development of a novel, CNS-penetrant, metabotropic glutamate receptor 3 (mGlu3) NAM probe (ML289) derived from a closely related mGlu5 PAM. *Bioorg. Med. Chem. Lett.* 22, 3921–3925.

- (17) Gregory, K. J., Nguyen, E. D., Reiff, S. D., Squire, E. F., Stauffer, S. R., Lindsley, C. W., Meiler, J., and Conn, P. J. (2013) Probing the

metabotropic glutamate receptor 5 (mGlu5) positive allosteric modulator (PAM) binding pocket: discovery of point mutations that engender a “molecular switch” in PAM pharmacology. *Mol. Pharmacol.* 83, 991–1006.

(18) Malherbe, P., Kratochwil, N., Muhlemann, A., Zenner, M.-T., Fischer, C., Stahl, M., Gerber, P. R., Jaeschke, G., and Porter, R. H. P. (2006) Comparison of the binding pockets of two chemically unrelated allosteric antagonists of the mGlu5 receptor and identification of crucial residues involved in the inverse agonism of MPEP. *J. Neurochem.* 98, 601–615.

(19) Malherbe, P., Kratochwil, N., Zenner, M. T., Piussi, J., Diener, C., Kratzeisen, C., Fischer, C., and Porter, R. H. (2003) Mutational analysis and molecular modeling of the binding pocket of the metabotropic glutamate 5 receptor negative modulator 2-methyl-6-(phenylethynyl)-pyridine. *Mol. Pharmacol.* 64, 823–832.

(20) Molck, C., Harpsoe, K., Gloriam, D. E., Clausen, R. P., Madsen, U., Pedersen, L. O., Jimenez, H. N., Nielsen, S. M., Mathiesen, J. M., and Brauner-Osborne, H. (2012) Pharmacological Characterization and Modeling of the Binding Sites of Novel 1,3-bis(pyridinylethynyl)-benzenes as Metabotropic Glutamate Receptor 5-selective Negative Allosteric Modulators. *Mol. Pharmacol.* 82, 929–937.

(21) Muhlemann, A., Ward, N. A., Kratochwil, N., Diener, C., Fischer, C., Stucki, A., Jaeschke, G., Malherbe, P., and Porter, R. H. (2006) Determination of key amino acids implicated in the actions of allosteric modulation by 3,3'-difluorobenzaldazine on rat mGlu5 receptors. *Eur. J. Pharmacol.* 529, 95–104.

(22) Pagano, A., Ruegg, D., Litschig, S., Stoehr, N., Stierlin, C., Heinrich, M., Floersheim, P., Prezeau, L., Carroll, F., Pin, J. P., Cambria, A., Vranesic, I., Flor, P. J., Gasparini, F., and Kuhn, R. (2000) The non-competitive antagonists 2-methyl-6-(phenylethynyl)pyridine and 7-hydroxyiminocyclopropan[b]chromen-1a-carboxylic acid ethyl ester interact with overlapping binding pockets in the transmembrane region of group I metabotropic glutamate receptors. *J. Biol. Chem.* 275, 33750–33758.

(23) Turlington, M., Noetzel, M. J., Chun, A., Zhou, Y., Gogliotti, R. D., Nguyen, E. D., Gregory, K. J., Vinson, P. N., Rook, J. M., Gogi, K. K., Xiang, Z., Bridges, T. M., Daniels, J. S., Jones, C., Niswender, C. M., Meiler, J., Conn, P. J., Lindsley, C. W., and Stauffer, S. R. (2013) Exploration of Allosteric Agonism Structure-Activity Relationships within an Acetylene Series of Metabotropic Glutamate Receptor 5 (mGlu5) Positive Allosteric Modulators (PAMs): Discovery of 5-((3-Fluorophenyl)ethynyl)-N-(3-methyloctan-3-yl)picolinamide (ML254). *J. Med. Chem.* 56, 7976–7996.

(24) Cosford, N. D., Roppe, J., Tehrani, L., Schweiger, E. J., Seiders, T. J., Chaudary, A., Rao, S., and Varney, M. A. (2003) [3H]-methoxymethyl-MTEP and [3H]-methoxy-PEPy: potent and selective radioligands for the metabotropic glutamate subtype 5 (mGlu5) receptor. *Bioorg. Med. Chem. Lett.* 13, 351–354.

(25) Gregory, K. J., Noetzel, M. J., Rook, J. M., Vinson, P. N., Stauffer, S. R., Rodriguez, A. L., Emmitte, K. A., Zhou, Y., Chun, A. C., Felts, A. S., Chauder, B. A., Lindsley, C. W., Niswender, C. M., and Conn, P. J. (2012) Investigating Metabotropic Glutamate Receptor 5 Allosteric Modulator Cooperativity, Affinity and Agonism: Enriching Structure-function Studies and Structure-activity Relationships. *Mol. Pharmacol.* 82, 860–875.

(26) Mueller, R., Dawson, E. S., Meiler, J., Rodriguez, A. L., Chauder, B. A., Bates, B. S., Felts, A. S., Lamb, J. P., Menon, U. N., Jadhav, S. B., Kane, A. S., Jones, C. K., Gregory, K. J., Niswender, C. M., Conn, P. J., Olsen, C. M., Winder, D. G., Emmitte, K. A., and Lindsley, C. W. (2012) Discovery of 2-(2-Benzoxazolyl amino)-4-Aryl-5-Cyanopyrimidine as Negative Allosteric Modulators (NAMs) of Metabotropic Glutamate Receptor 5 (mGlu5): From an Artificial Neural Network Virtual Screen to an In Vivo Tool Compound. *ChemMedChem* 7, 406–414.

(27) Kulkarni, S. S., Zou, M. F., Cao, J., Deschamps, J. R., Rodriguez, A. L., Conn, P. J., and Newman, A. H. (2009) Structure-activity relationships comparing N-(6-methylpyridin-yl)-substituted aryl amides to 2-methyl-6-(substituted-arylethynyl)pyridines or 2-methyl-

4-(substituted-arylethynyl)thiazoles as novel metabotropic glutamate receptor subtype 5 antagonists. *J. Med. Chem.* 52, 3563–3575.

(28) Alagille, D., Baldwin, R. M., Roth, B. L., Wroblewski, J. T., Grajkowska, E., and Tamagnan, G. D. (2005) Synthesis and receptor assay of aromatic-ethynyl-aromatic derivatives with potent mGluR5 antagonist activity. *Bioorg. Med. Chem.* 13, 197–209.

(29) Zou, M. F., Cao, J., Rodriguez, A. L., Conn, P. J., and Newman, A. H. (2011) Design and synthesis of substituted N-(1,3-diphenyl-1H-pyrazol-5-yl)benzamides as positive allosteric modulators of the metabotropic glutamate receptor subtype 5. *Bioorg. Med. Chem. Lett.* 21, 2650–2654.

(30) Felts, A. S., Rodriguez, A. L., Morrison, R. D., Venable, D. F., Manka, J. T., Bates, B. S., Blobaum, A. L., Byers, F. W., Daniels, J. S., Niswender, C. M., Jones, C. K., Conn, P. J., Lindsley, C. W., and Emmitte, K. A. (2013) Discovery of VU0409106: A negative allosteric modulator of mGlu5 with activity in a mouse model of anxiety. *Bioorg. Med. Chem. Lett.* 23, 5779–5785.

(31) Gregory, K. J., Herman, E. J., Ramsey, A. J., Hammond, A. S., Byun, N. E., Stauffer, S. R., Manka, J. T., Jadhav, S., Bridges, T. M., Weaver, C. D., Niswender, C. M., Steckler, T., Drinkenburg, W. H., Ahnaou, A., Lavreysen, H., Macdonald, G. J., Bartolome, J. M., Mackie, C., Hrupka, B. J., Caron, M. G., Daigle, T. L., Lindsley, C. W., Conn, P. J., and Jones, C. K. (2013) N-Aryl piperazine metabotropic glutamate receptor 5 positive allosteric modulators possess efficacy in pre-clinical models of NMDA hypofunction and cognitive enhancement. *J. Pharmacol. Exp. Ther.* 347, 438–457.

(32) Spear, N., Gadiant, R. A., Wilkins, D. E., Do, M., Smith, J. S., Zeller, K. L., Schroeder, P., Zhang, M., Arora, J., and Chhajlani, V. (2011) Preclinical profile of a novel metabotropic glutamate receptor 5 positive allosteric modulator. *Eur. J. Pharmacol.* 659, 146–154.

(33) Xiong, H., Brugel, T. A., Balestra, M., Brown, D. G., Brush, K. A., Hightower, C., Hinkley, L., Hoesch, V., Kang, J., Koether, G. M., McCauley, J. P., Jr., McLaren, F. M., Panko, L. M., Simpson, T. R., Smith, R. W., Woods, J. M., Brockel, B., Chhajlani, V., Gadiant, R. A., Spear, N., Sygowski, L. A., Zhang, M., Arora, J., Breyse, N., Wilson, J. M., Isaac, M., Slassi, A., and King, M. M. (2010) 4-aryl piperazine and piperidine amides as novel mGluR5 positive allosteric modulators. *Bioorg. Med. Chem. Lett.* 20, 7381–7384.

(34) Chen, Y., Nong, Y., Goudet, C., Hemstapat, K., de Paulis, T., Pin, J. P., and Conn, P. J. (2007) Interaction of novel positive allosteric modulators of metabotropic glutamate receptor 5 with the negative allosteric antagonist site is required for potentiation of receptor responses. *Mol. Pharmacol.* 71, 1389–1398.

(35) de Paulis, T., Hemstapat, K., Chen, Y., Zhang, Y., Saleh, S., Alagille, D., Baldwin, R. M., Tamagnan, G. D., and Conn, P. J. (2006) Substituent effects of N-(1,3-diphenyl-1H-pyrazol-5-yl)benzamides on positive allosteric modulation of the metabotropic glutamate-5 receptor in rat cortical astrocytes. *J. Med. Chem.* 49, 3332–3344.

(36) Kinney, G. G., O'Brien, J. A., Lemaire, W., Burno, M., Bickel, D. J., Clements, M. K., Chen, T. B., Wisnoski, D. D., Lindsley, C. W., Tiller, P. R., Smith, S., Jacobson, M. A., Sur, C., Duggan, M. E., Pettibone, D. J., Conn, P. J., and Williams, D. L., Jr. (2005) A novel selective positive allosteric modulator of metabotropic glutamate receptor subtype 5 has in vivo activity and antipsychotic-like effects in rat behavioral models. *J. Pharmacol. Exp. Ther.* 313, 199–206.

(37) Kaae, B. H., Harpsoe, K., Kvist, T., Mathiesen, J. M., Molck, C., Gloriam, D., Jimenez, H. N., Uberti, M. A., Nielsen, S. M., Nielsen, B., Brauner-Osborne, H., Sauerberg, P., Clausen, R. P., and Madsen, U. (2012) Structure-activity relationships for negative allosteric mGluR5 modulators. *ChemMedChem* 7, 440–451.

(38) Deupi, X., and Standfuss, J. (2011) Structural insights into agonist-induced activation of G-protein-coupled receptors. *Curr. Opin. Struct. Biol.* 21, 541–551.

(39) Ortiz, A. R., Strauss, C. E., and Olmea, O. (2002) MAMMOTH (matching molecular models obtained from theory): an automated method for model comparison. *Protein Sci.* 11, 2606–2621.

(40) Nguyen, E. D., Norn, C., Frimurer, T. M., and Meiler, J. (2013) Assessment and challenges of ligand docking into comparative models of G-protein coupled receptors. *PLoS One* 8, e67302.

- (41) Tautermann, C. S., and Pautsch, A. (2011) The Implication of the First Agonist Bound Activated GPCR X-ray Structure on GPCR in Silico Modeling. *ACS Med. Chem. Lett.* 2, 414–418.
- (42) Felts, A. S., Lindsley, S. R., Lamb, J. P., Rodriguez, A. L., Menon, U. N., Jadhav, S., Jones, C. K., Conn, P. J., Lindsley, C. W., and Emmitte, K. A. (2010) 3-Cyano-5-fluoro-N-arylbenzamides as negative allosteric modulators of mGlu(5): Identification of easily prepared tool compounds with CNS exposure in rats. *Bioorg. Med. Chem. Lett.* 20, 4390–4394.
- (43) Labute, P. (2010) LowModeMD—implicit low-mode velocity filtering applied to conformational search of macrocycles and protein loops. *J. Chem. Inf. Model.* 50, 792–800.
- (44) Davis, I. W., and Baker, D. (2009) RosettaLigand docking with full ligand and receptor flexibility. *J. Mol. Biol.* 385, 381–392.
- (45) Lemmon, G., and Meiler, J. (2012) Rosetta Ligand docking with flexible XML protocols. *Methods Mol. Biol.* 819, 143–155.
- (46) Meiler, J., and Baker, D. (2006) ROSETTALIGAND: protein-small molecule docking with full side-chain flexibility. *Proteins* 65, 538–548.
- (47) Roppe, J., Smith, N. D., Huang, D., Tehrani, L., Wang, B., Anderson, J., Brodtkin, J., Chung, J., Jiang, X., King, C., Munoz, B., Varney, M. A., Prasit, P., and Cosford, N. D. (2004) Discovery of novel heteroarylazoles that are metabotropic glutamate subtype 5 receptor antagonists with anxiolytic activity. *J. Med. Chem.* 47, 4645–4648.
- (48) Alagille, D., Baldwin, R. M., Roth, B. L., Wroblewski, J. T., Grajkowska, E., and Tamagnan, G. D. (2005) Functionalization at position 3 of the phenyl ring of the potent mGluR5 noncompetitive antagonists MPEP. *Bioorg. Med. Chem. Lett.* 15, 945–949.